AIP Conference Proceedings

Determining the Young’s modulus of a cellular titanium implant by FEM simulation

Cite as: AIP Conference Proceedings **1915**, 030010 (2017); https://doi.org/10.1063/1.5017330
Published Online: 12 December 2017

Yu. N. Loginov, A. I. Golodnov, S. I. Stepanov, and E. Yu. Kovalev

View Online
Export Citation

ARTICLES YOU MAY BE INTERESTED IN

Effect of strain rate on the formation of the microstructure of a 1950/10% SiC metal matrix composite under high temperature
AIP Conference Proceedings **1915**, 030002 (2017); https://doi.org/10.1063/1.5017322

Surface stress on the effective Young’s modulus and Poisson’s ratio of isotropic nanowires under tensile load
AIP Advances **5**, 117206 (2015); https://doi.org/10.1063/1.4935439

Research of the stress-strain state of rods obtained by porous blank extrusion
AIP Conference Proceedings **1915**, 030003 (2017); https://doi.org/10.1063/1.5017323

© 2017 Author(s).

Determining the Young's Modulus of a Cellular Titanium Implant by FEM Simulation

Yu. N. Loginov[a)], A. I. Golodnov[b)], S. I. Stepanov[c)] and E. Yu. Kovalev[d)]

Ural Federal University named after the 1st President of Russia B. N. Yeltsin, 19 Mira St., Eekaterinburg, 620002, Russia

[a)]j.n.loginov@urfu.ru
[b)]a.i.golodnov@urfu.ru
[c)]Corresponding author: s.i.stepanov@urfu.ru
[d)]cska.93.93@mail.ru

Abstract. The role of additive manufacturing is noted for the construction of titanium medical implants. The purpose of the study is to determine the Young's modulus of cellular titanium implants, which is based on calculations performed by finite element analysis. A honeycomb structure from intersecting cylinder surfaces is offered for the implant made of the Ti-6Al-4V alloy. Boundary conditions are stated for the loading of the implant structure. It is demonstrated that the Young's modulus can be reduced more than three times comparing to a solid titanium alloy. Zones of strain and stress localization located near the abutment of the cylindrical surfaces. Recommendations for the further improvement of the implant architecture are generated.

INTRODUCTION

Recently, additive manufacturing has come to the fore as a universal approach to the fabrication of porous titanium implants for surgery applications [1]. These technologies allow one to design objects with tailored architecture – internal and external structure. The Young's modulus is one of the implant parameters, which is to be tailored based on the optimal strength to rigidity ratio of the structure [2]. In order to determine the Young's modulus, experimental methods and techniques are utilized based on the phase composition [3], texture [4] and pore (cell) architecture [5]. Note that the Young's modulus depends not only on the structure porosity. The shape and distribution of pores in a honeycomb structure affect the elastic constant as well. Therefore, space architecture consisting of pores and struts has to be designed first. Then, the elasticity characteristics are determined and, if necessary, strength calculations are performed.

CALCULATION PROCEDURE

The honeycomb structure shown in Fig. 1a is used as a basic space architecture. The unit cell that forms this structure is a junction of three cylinders with a diameter of 1.2×10^{-3} m and a length of 2.1×10^{-3} (Fig. 1b).

The implant porosity P is estimated in % by the formula

$$P = (1 - \frac{\rho_v}{\rho_t}) \cdot 100\ \%, \tag{1}$$

where ρ_υ and ρ_t are the density of the honeycomb structure and the density of the solid material from which the implant was manufactured, respectively, while

Mechanics, Resource and Diagnostics of Materials and Structures (MRDMS-2017)
AIP Conf. Proc. 1915, 030010-1–030010-4; https://doi.org/10.1063/1.5017330
Published by AIP Publishing. 978-0-7354-1607-9/$30.00

$$\rho_V = \frac{m}{V}, \tag{2}$$

m and V are the weight and volume of the implant with pores.

Using the Solid Works software, a 3D unit cell for the Young's modulus simulation is designed. The Ti-6Al-4V titanium alloy, with a density of 4430 kg/m^3 is used as a basic modeling material for calculations, since it is generally used to manufacture implants. The weight of the unit cell is 2.07×10^{-5} kg according to the data of Solid Works. Since the unit cell is inscribed in a cube with a side length of 2.1×10^{-3} m, the cell volume with pores is $(2.1\times10^{-3})^3 = 9.261\times10^{-9}$ m^3, which, in accordance with formula (2), leads to the result $\rho_v = \frac{2.07\times10^{-5}}{9.261\times10^{-9}} 2235 kg/m^3$ and, by formula (1), we obtain $P = (1-\frac{2235}{4430})\cdot 100 = 49.5\%$.

The compressive loading is simulated by means of finite element analysis (FEA) using the ANSYS module Mechanical Structure. The properties of the alloy are given by the following constants: a density of 4430 kg/m^3, a Young's modulus of 114 GPa, a Poisson's ratio of 0.342, a yield tensile and compressive strength of 780 MPa, an ultimate tensile strength of 900 MPa and an ultimate compressive strength of 110 MPa.

(a) (b)

FIGURE 1. Cellular architecture of the implant (a) and a separate unit cell (b)

A quarter of a unit cell is identified as the initial model to simplify the problem, since the unit cell consists of four identical parts cyclically repeating around the vertical Y-axis of the orthogonal coordinate system XYZ. A graphical representation of the loading conditions and the boundary conditions is shown in Fig. 2a.

(a) (b)

FIGURE 2. Schematic boundary conditions of loading (a) and a unit cell meshed into hexagonal finite elements (b)

According to the problem conditions, the unit cell is subjected to a constant pressure of 10 MPa (marked with arrows) along the Y-axis. Such loading conditions are chosen to provide the elastic material behavior and to avoid plastic deformation under the applied pressure.

The pressure is transferred to the cell through a square plate with a side of the square of 1.05×10^{-3} m and a thickness of 2×10^{-4} m. The material of the plate is characterized by a preset huge elastic modulus of 250,000 GPa, so that it can be considered as a completely rigid body. The displacement of the lower base of the unit cell in the direction of the *Y*-axis is set equal to zero, while the condition of the absence of friction is specified in the *ZX* plane. Zero friction is set between the plate and the unit cell as well. The *XY* and *YZ* planes are considered as planes of symmetry; thus, horizontal displacement *UX* in the *YZ* plane and *UZ* displacement in the *XY* plane were equal to zero.

A structured hexagonal mesh with the minimal size of the elementary cell of 2.5×10^{-5} is taken for simulation in ICEM CFD of the ANSYS software (Fig. 1b). The quality of the mesh is estimated using the Element Quality composite quality measure. This indicator varies from 0.35091 to 0.99923 with an average value of 0.82358, which corresponds to the recommendations (not lower than 0.3) provided by the software.

RESULTS AND DISCUSSION

The distribution of the characteristics of the stress-strain state is obtained by simulation of loading for a quarter of the unit cell shown in Figs. 3 and 4. The strain along the loading *Y*-axis (Fig. 3a) is required to determine the elastic modulus. As can be seen from the figure, the largest displacement is achieved for the upper plane of the cell, and it is equal to $-6.08*10^{-7}$ mm. The areas of the equal levels of displacements in the *Y*-direction are obtained (Fig. 3a, b) according to the simulation for the unit cell of the honeycomb structure and the regions of the equal levels of equivalent elastic strain (Fig. 4a, b).

The Young's modulus *E* is estimated by the formula

$$E = \frac{\sigma}{\varepsilon}, \tag{3}$$

where σ is normal stress applied to the honeycomb structure; ε is the strain of the honeycomb structure under the applied stress,

$$\varepsilon = \frac{\Delta}{l}, \tag{4}$$

where Δ is the displacement of the upper plane of the unit cell; *l* is the unit cell height.

Assuming σ = 10 MPa and $l = 2.1\times10^{-3}$ m and calculating Δ equal to 6.08×10^{-7} m, we obtain $\varepsilon = \frac{6.08\times10^{-7}}{2.1\times10^{-3}} = 2.895\times10^{-4}$ and the elastic modulus $E = \frac{10^7}{2.895\times10^{-4}} = 3.45\times10^{10}$ Pa, or 34.5 GPa. A comparison with the elastic modulus of the alloy from which the implant was made (114 GPa) shows that it is possible to reduce the initial module more than three times.

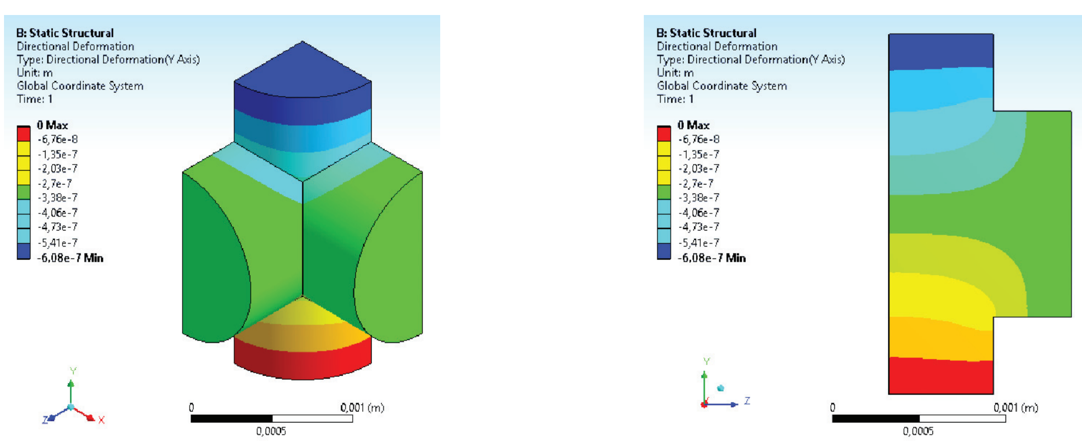

(a) (b)

FIGURE 3. Projection of the displacement vector *Uy* for the isometric view of the unit cell (a) and in the *ZY*-plane (b).

Zones of equivalent strain localization resulting from loading are shown in Fig. 4a, b. They are located in the intersection of the cylindrical struts. The simulation has shown that the maximum equivalent stress occurs in these regions. Thus, these regions serve as dangerous sections. The implant design can be improved by creating the binding radial surfaces, which provide smooth transition between the intersecting cylindrical surfaces. This enables us to rectify the peaks of equivalent stress and to prevent stress localization, as is known from the theory of elasticity.

It can also be supposed that the variation of the length of the intersecting cylinders results in the porosity of the honeycomb structure and in the alteration of the elastic and strength characteristics.

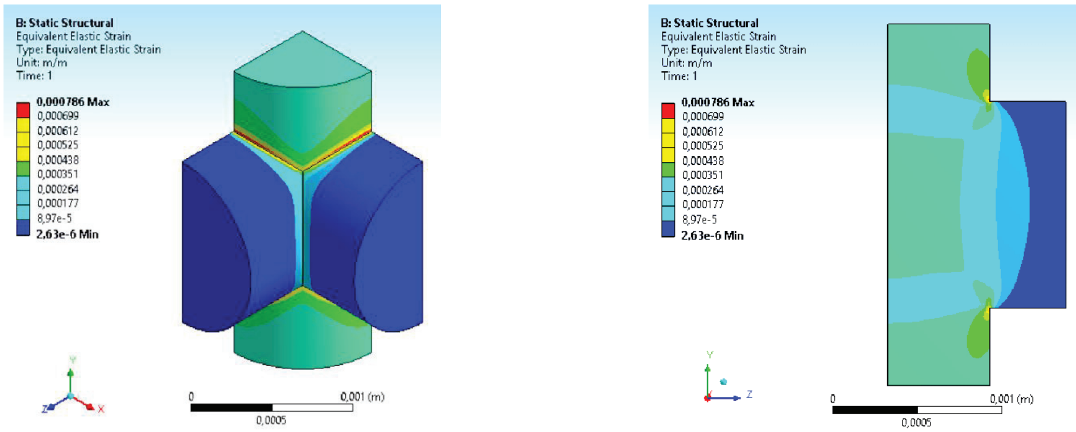

(a) (b)

FIGURE 4. Equivalent elastic strain field ε for the isometric view of the unit cell (a) and in the *ZY*-plane (b) for loading along the *Y*-axis.

CONCLUSION

Thus, the evaluation of the elastic properties of the honeycomb structures of medical implants can be made by FEA simulation. In this study, the honeycomb structure has been simulated for an implant with a more than three times decreased Young's modulus as compared to a solid titanium alloy. Zones with localized equivalent strains and stresses are located in the regions of surface abutment of cylindrical struts. The recommendations for possible improvement of the implant architecture have been developed.

ACKNOWLEDGMENTS

We hereby acknowledge the support of the Ministry of Science and Education of the Russian Federation, in accordance with the decree of the Government of April 9, 2010, No. 218, project number 03.G25.31.0234.

REFERENCES

1. F. Li, J. Li, H. Kou and L. Zhou, Materials Science and Engineering: C **60**, 485–488 (2016).
2. I. Tsukrov and J. Novak, International Journal of Solids and Structures **39**, 1539–1555 (2002).
3. S. V. Grib, A. G. Illarionov, A. A. Popov and O. M. Ivasishin, The Physics of Metals and Metallography **115**, 600–608 (2014).
4. P. P. Pal-Val, Yu. N. Loginov, S. L. Demakov, A. G. Illarionov, V. D. Natsik, L. N. Pal-Val, A. A. Davydenko and A. P. Rybalko, Materials Science and Engineering A **618**, 9–15 (2014).
5. H. Shen, H. Li and L. C. Brinson, Mechanics of Materials **40**, 708–720 (2008).